A study of the structural and catalytic effects of sulfation on iron oxide catalysts prepared from goethite and ferrihydrite precursors for methane oxidation

A.S.C. Brown, J.S.J. Hargreaves and B. Rijniersce

Catalysis Research Laboratory, Department of Chemistry and Physics, Nottingham Trent University, Clifton Lane, Nottingham, NG11 8NS, UK

Received 29 January 1998; accepted 3 April 1998

A study of the effects of sulfation on the methane oxidation activity of iron oxide catalysts prepared from goethite and 2-line ferrihydrite precursors is presented. Although catalytic performance is found to be dependent upon the precursor, sulfation produces general effects in both systems. Surface area is increased, oxidation activity $<400\,^{\circ}C$ is suppressed, and that at $500\,^{\circ}C$ is enhanced leading to the production of selective products. Despite these similarities, sulfation produces different structural effects in the two systems. In the case of iron oxide prepared from goethite, extensive pitting and an increase in disorder in the cationic arrangement are observed. In contrast, a slight increase in crystallinity of the iron oxide prepared from ferrihydrite occurs. The effect of sulfation on catalytic performance is interpreted in terms of a two-site mechanism, complexation poisoning Fe^{3+} sites active for the lower-temperature oxidation activity with additional sites active at higher temperature being produced.

Keywords: sulfated iron oxide, methane oxidation, goethite, ferrihydite, haematite

1. Introduction

In recent years, considerable research attention has been directed towards a number of sulfated metal oxide systems primarily because of their ability to catalyse alkane isomerisation reactions at low temperatures [1]. In such systems, it has been demonstrated that the method of preparation is of crucial importance. It has generally been reported that sulfation should be performed using a reagent such as sulfuric acid or ammonium sulfate on the oxide precursor – usually the hydroxide or oxyhydroxide – which is subsequently dried and calcined to yield the active catalyst. The temperature of calcination to produce the most active materials is dependent upon the oxide and, also, the sulfation reagent. It has been proposed that the properties of such materials are related to the development of "superacidity", although this is currently a subject of debate [2,3]. On the basis of spectroscopic measurements and isotopic reaction studies, Adeeva et al. [2] have argued that the high activity of sulfated zirconia for butane isomerisation is due to the ability of sulfate to stabilise surface transition states, and Farcasiu and co-workers [3] have presented arguments for the role of sulfate as a one-electron oxidant.

The vast majority of effort to date has been directed towards the isomerisation activity of sulfated zirconia and related materials [4]. In this study, we turn our attention towards the methane oxidation properties of the sulfated iron oxide system. Our interest in this area arises from the potential of combining the hydrocarbon activation properties of sulfated systems with the redox behaviour of iron oxide. In principle, this combination could lead to the potential of circumventing the gas-phase limitations known to be operative in direct partial oxidation systems [5], or of producing effective low-temperature combustion catalysts.

To date, there have only been few studies of methane activation over sulfated metal oxides published. Lin and Hsu have commented that their sulfated iron manganese zirconia catalyst was effective for the non-oxidative conversion of methane to ethane below $300\,^{\circ}C$ [6], and Murata et al. [7] have recently reported that lithium-doped sulfated zirconia is an effective catalyst for the oxidative coupling of methane. In that study, sulfation alone was reported to have little effect on the catalytic performance of zirconia at $800\,^{\circ}C$, however. Batamack and co-workers [8] have reported that systems based on sulfated zirconia are effective catalysts for methane chlorination below $240\,^{\circ}C$. It was considered that reaction occurred via the intermediacy of electrophilic chlorine species generated on zirconium cations in close proximity with sulfate species.

In the following, we describe our preliminary studies on the characterisation and catalytic properties on sulfated iron oxide derived from two very different precursors – goethite and 2-line ferrihydrite.

2. Experimental

2.1. Catalyst preparation

(i) Goethite – 100 ml of a 1 M solution of iron(III) nitrate nonahydrate (Avocado 98+%) prepared using distilled water was added to a polythene screwtop bottle. To this, 180 ml of a 5 M sodium hydroxide solution was added with stirring. This solution was then diluted to 500 ml with distilled water

and aged in an oven at 70 °C for sixty hours. The resultant yellow precipitate was then filtered and washed with 4 l of distilled water and dried in a vacuum oven for two days. Powder X-ray diffraction confirmed that this material was goethite.

(ii) 2-line ferrihydrite – 40 g of iron(III) nitrate nonahydrate (Fisons 98+%) was dissolved in 500 ml of distilled water. 330 ml of 1 M sodium hydroxide solution was added with stirring to raise the pH to 7.5, with the last 20 ml being added dropwise. The material was then filtered, washed with 2.5 l of distilled water and dried at 100 °C over night. The powder X-ray diffraction pattern of this material was consistent with 2-line ferrihydrite.

(iii) Sulfated iron oxides – 2 g of the oxide precursor was immersed in 30 ml of 0.5 M sulfuric acid for thirty minutes. The solution was then filtered and the filtrate was dried at 100 °C overnight. The material was then calcined at 550 °C for three hours in static air and was pelleted and sieved (0.6–1.0 mm particles) prior to activity testing. The material prepared from goethite precursor is designated SO_4^{2-}/Fe_2O_3(G) and that from ferrihydrite SO_4^{2-}/Fe_2O_3(F) in the following.

(iv) H_2O/Fe_2O_3 (G) and (F) – these materials were prepared in an analogous manner to their sulfated counterparts, except that immersion was performed in distilled water.

(v) α-Al_2O_3 (Aldrich, 99%) was pelleted and sieved (0.6–1.0 mm particles) prior to activity testing.

2.2. Catalyst testing

Catalyst performance was evaluated in a fixed-bed catalytic microreactor operating at 15 bar pressure. A stainless steel jacketed quartz reactor tube (8.5 mm ID) was used in which 0.75 ml of catalyst (which corresponded to ca. 0.5–0.6 g) was held centrally in the heated zone of a tube furnace between quartz wool plugs. Methane (Air Products, 99%), oxygen (Air Products, 99.6%) and helium (Air Products, 99.999%) were fed to the reactor in the ratio $46:4:12$ ml min^{-1} to give a GHSV of $\sim$4600 h^{-1}. The flow rates were maintained with Brooks mass-flow controllers, and the pressure with a Tescom back-pressure regulator. All lines downstream of the reactor were trace heated to a temperature in excess of 150 °C to prevent condensation of the products. Analysis was performed on-line using a Varian Saturn GCMS equipped with thermal-conductivity detector. Megabore Poraplot GS-Q and Molesieve columns were used to effect the separation. The reactor was allowed to stabilise for one hour prior to data collection, and the results reported are the mean of three analyses.

2.3. Catalyst characterisation

Surface area determination was performed by the BET method using nitrogen physisorption.

Transmission electron microscopy was performed using a Jeol 2010 electron microscope operating at 200 keV. Samples were prepared by sprinkling onto carbon-coated copper grids and removing the excess by shaking.

Powder X-ray diffraction studies were performed on a Hiltonbrooks modified Phillips powder diffractometer fitted with detector monochromator. Cu K_α radiation was used with the X-ray generator operating at 40 kV and 20 mA. Samples were prepared by compaction into an aluminium sample holder and were scanned in the range 5–75° 2θ at a step size of 0.05° and counting rate of 2°/min.

FTIR studies were performed on samples in the form of KBr discs using a Perkin-Elmer 1600 series spectrometer operating at 4 cm^{-1} resolution.

3. Results and discussion

Table 1 presents the results of methane oxidation studies. α-Al_2O_3 has been included because it is considered to be inert and, therefore, indicates the background activity which is known to be significant for this reaction [9]. On inspection of the data, it is apparent that all the iron oxide materials possess activity in excess of the background. Furthermore, there are a number of interesting features. The catalytic performance of the materials relates to their precursor. Iron oxides produced from ferrihydrite were less active than their counterparts produced from goethite although having higher surface area. Despite these differences, the effects of sulfation were observed to be generally similar between the two systems. Sulfation increased surface area, suppressed low-temperature total oxidation and enhanced the production of selective oxidation products (ethane and methanol) at 500 °C – the methanol space time yields for both systems are in the range of 20–30 $g_{CH_3OH}\,kg_{cat}^{-1}\,h^{-1}$. The magnitude of the enhancement of activity appears to vary with the precursor, sulfation clearly producing an increase in specific activity in the case of the ferrihydrite-derived material but not for goethite, which, nevertheless, still exhibits the higher specific activity. This comparison should be treated with caution, however, since we have observed that the absolute performance of sulfated materials is difficult to reproduce, unlike the general trends. This phenomenon, which may relate to differences in sulfation level and/or precursor age, is currently being investigated. Others have noted that the reproducibility of sulfation of zirconia with sulfuric acid is low [10], and an improved preparation method has recently been reported [11].

To determine whether the effects noted above are structural/morphological in nature, the iron oxides have been characterised by a combination of transmission electron microscopy and powder X-ray diffraction. Figure 1 presents transmission electron micrographs of the goethite precursor, H_2O/Fe_2O_3(G) and SO_4^{2-}/Fe_2O_3(G), as prepared. The needle-shaped crystals shown in figure 1(a) are characteristic of those published in the literature for acicular goethite [12]. Figure 1 (b) and (c) shows that this general form of morphology has been maintained in the H_2O/Fe_2O_3(G) and SO_4^{2-}/Fe_2O_3(G) materials, although some growth has occurred along the needle axis (from ca. 0.5 to ca. 1 μm). Powder X-ray diffraction confirmed that

Table 1
Catalytic results for α-Al_2O_3, sulfated and non-sulfated iron oxide samples.

Sample	Surface area (m^2/g)	Temperature (°C)	Conversion (%)		Selectivity[a] (%)			
			CH_4	O_2	CO_2	CO	C_2H_6	CH_3OH
α-Al_2O_3	–	300	–	–	–	–	–	–
		400	–	–	–	–	–	–
		500	0.6	12.9	100	–	–	–
H_2O/Fe_2O_3(G)	13	300	0.1	1.3	100	–	–	–
		400	4.0	73.5	100	–	–	–
		500	5.6	71.9	89	11	–	–
SO_4^{2-}/Fe_2O_3(G)	29	300	–	–	–	–	–	–
		400	0.4	9.2	16	84	–	–
		500	5.9	85.0	32	61	3	4
H_2O/Fe_2O_3(F)	15	300	–	–	–	–	–	–
		400	0.7	16.5	100	–	–	–
		500	1.0	20.4	100	–	–	–
SO_4^{2-}/Fe_2O_3(F)	73	300	–	–	–	–	–	–
		400	–	–	–	–	–	–
		500	7.3	95.6	16	73	3	8

[a] Based on moles of carbon converted.

the precursor material was goethite and that both Fe_2O_3(G) samples were haematite. It has been reported elsewhere that the morphology of haematite may be related to that of its precursor when calcination is performed at the temperatures employed in this study [12]. It is interesting to note that sulfation has caused extensive pitting of the Fe_2O_3 needles which may, at least partly, explain the surface area differences between the two Fe_2O_3(G) samples. It is probable that pitting occurs via partial dissolution of the goethite precursor at domain boundaries, since previous work has shown that hole formation can occur in this region as a result of proton attack [13]. Figure 2 presents micrographs of the 2-line ferrihydrite precursor, H_2O/Fe_2O_3(F) and SO_4^{2-}/Fe_2O_3(F). There are major differences in comparison with the goethite system. As expected from its amorphous powder X-ray diffraction pattern, the precursor material is non-crystalline and is composed of very aggregated areas of material. Again, these findings are similar to those in previous studies of this material [12]. Both H_2O/Fe_2O_3(F) and SO_4^{2-}/Fe_2O_3(F) were observed to comprise highly aggregated crystallites with ill-defined morphology, and powder X-ray diffraction confirmed that these samples contained haematite. Interestingly, in this case the sulfation procedure was not observed to cause pitting.

The powder X-ray diffraction patterns of the Fe_2O_3 materials are shown in figures 3 and 4. As described above, all patterns match to haematite (JCPDS file number 13-534). Frequently, we observe additional reflections at ca. 45° and 65° 2θ, which we have been unable to assign yet. In the case of the ferrihydrite-derived materials, the very high backgrounds reflect the large degree of amorphous content. The inclusion of sulfate seems to have increased the crystallinity of the resultant haematite marginally despite increasing surface area. However, it is notable that fewer reflections are evident in the powder pattern, those at 45° and 65° 2θ are no longer present. For the Fe_2O_3(G) materials, it is interesting to note that the reflection widths are generally much larger for the SO_4^{2-}/Fe_2O_3(G), and that the differences in width are markedly anisotropic (table 2). On the basis of the comparative differences between the widths of the reflections, which indicate differences in the oxygen and iron sub-lattices [14], we propose that sulfation leads to poorer cationic ordering in the resultant haematite. It is probable that sulfate complexation hinders the topotactic goethite to haematite transformation by "pinning" iron ions. This transformation involves the loss of water and rearrangement of cations – the anionic frameworks are related, so comparatively little rearrangement of the oxygen lattice occurs [12]. Our FTIR studies of the sulfated goethite precursor reveal four stretches in the νS=O region (1226, 1137, 1077 and 996 cm^{-1}), which indicates sulfate complexation with a C_{2v} symmetry [15] and is consistent with assignments to chelating or cationic bridging forms [17]. The absence of such an anisotropic broadening effect in the diffraction patterns for the ferrihydrite-derived materials can be related to the observation that its transformation occurs by a different mechanism which, unlike goethite, does not seem to occur via the intermediacy of cationically disordered phases [17]. However, it is important to note that due to their amorphous nature, much less information on the ferrihydrite-derived materials can be obtained from the patterns, as the X-ray-detectable haematite is a minority phase. Sulfate also binds to ferrihydrite in a C_{2v} mode (νS=O 1208, 1132, 1061, 991 cm^{-1}), and our studies of SO_4^{2-}/Fe_2O_3(F) show that this symmetry is maintained in the resultant oxide. Studies in the literature have correlated the presence of C_{2v} symmetric sulfate with the superacidity/catalytic activity of sulfated oxides [18].

On the basis of the above observations, the most obvious explanation of the difference in catalytic activity be-

(a) 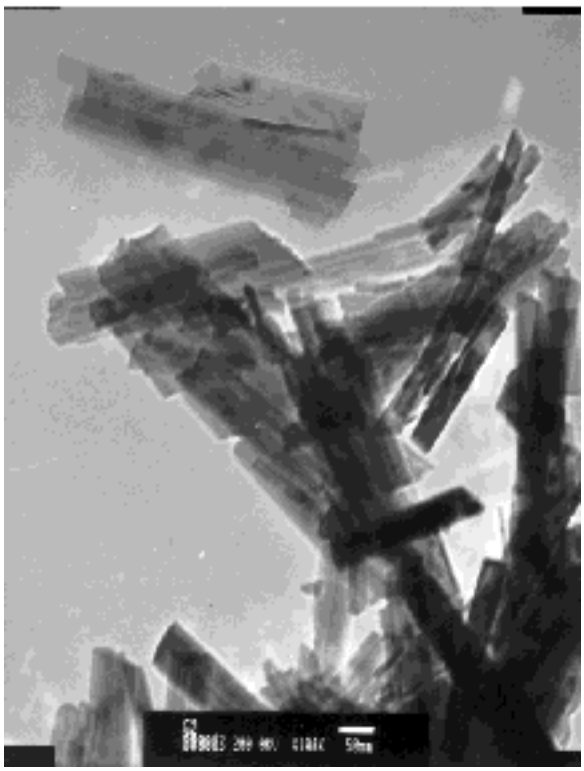

(b) 

(c) 

Figure 1. Transmission electron micrographs of (a) precursor goethite (magnification 100,000×), (b) H_2O/Fe_2O_3(G) (magnification 40,000×) and (c) SO_4^{2-}/Fe_2O_3(G) (magnification 60,000×).

(a)

(b)

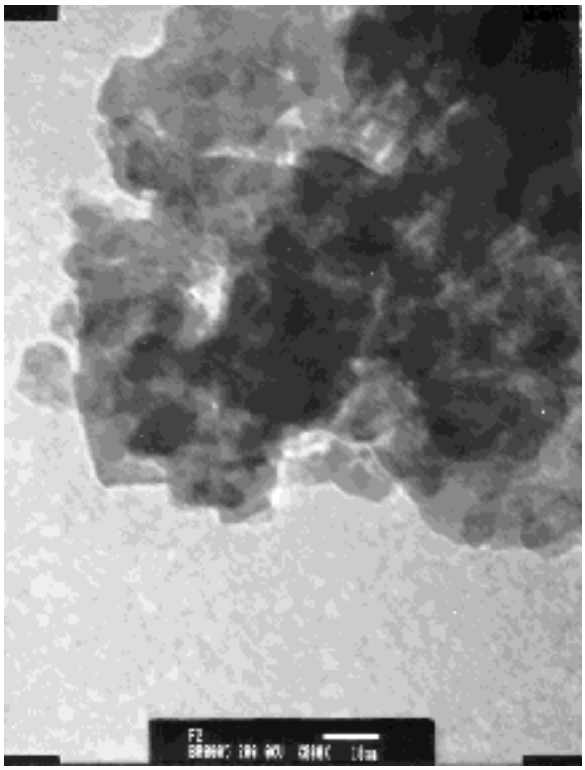

(c)

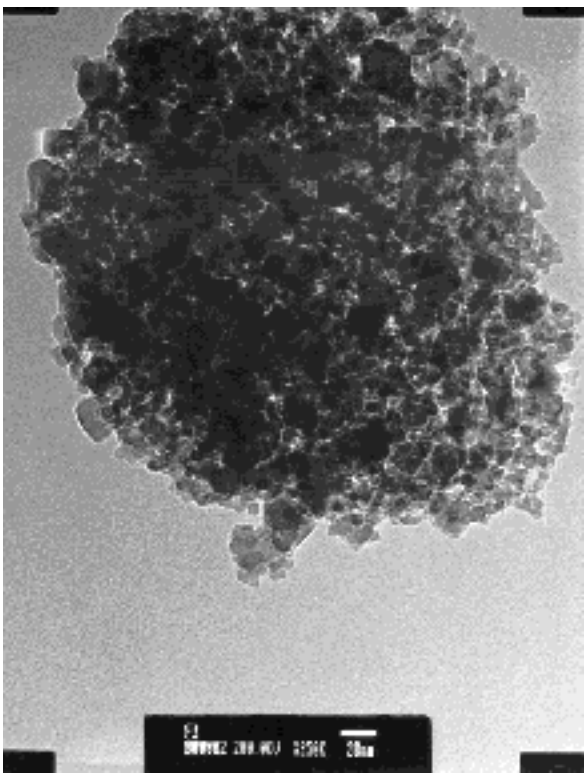

Figure 2. Transmission electron micrographs of (a) precursor 2-line ferrihydrite (magnification 250,000×), (b) H_2O/Fe_2O_3(F) (magnification 800,000×) and (c) SO_4^{2-}/Fe_2O_3(F) (magnification 250,000×).

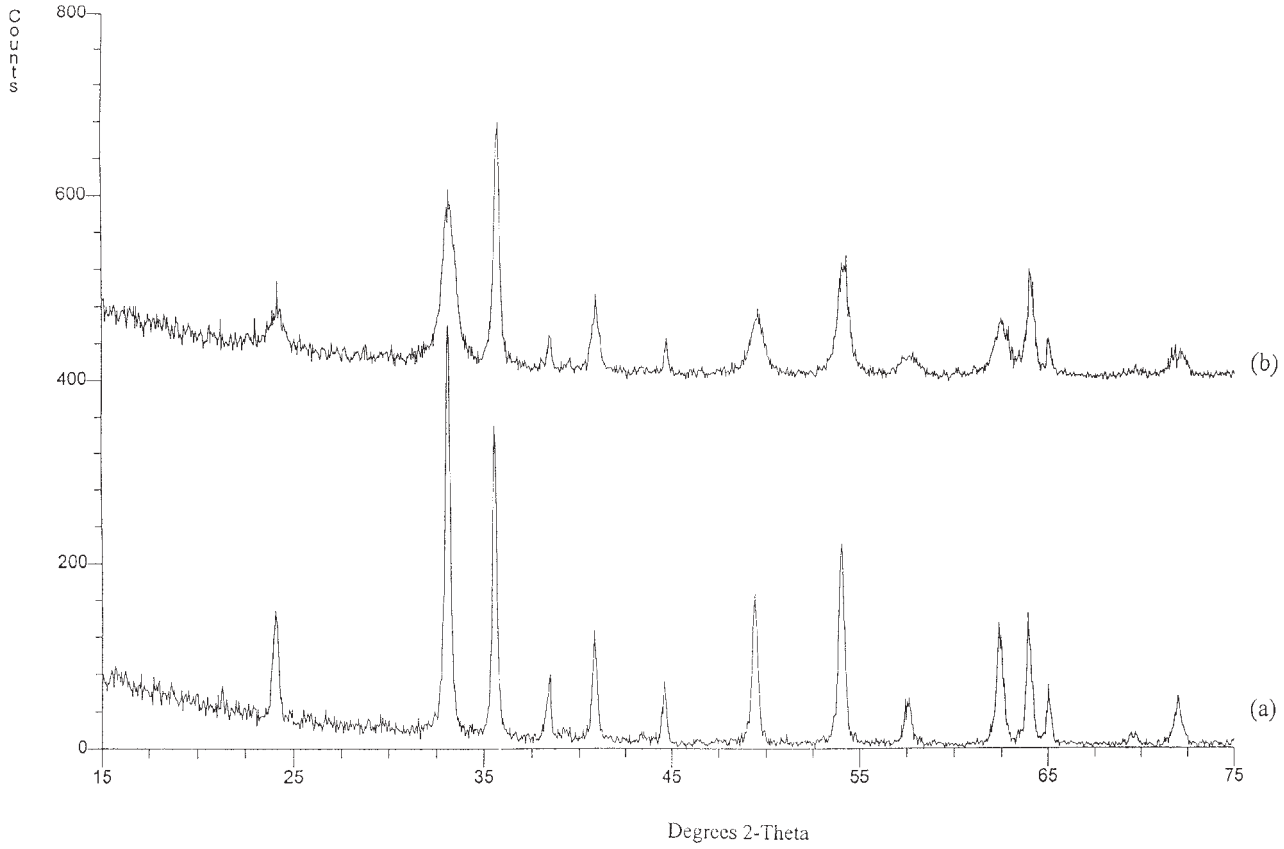

Figure 3. Powder X-ray diffraction pattern of (a) H_2O/Fe_2O_3(G) and (b) SO_4^{2-}/Fe_2O_3(G).

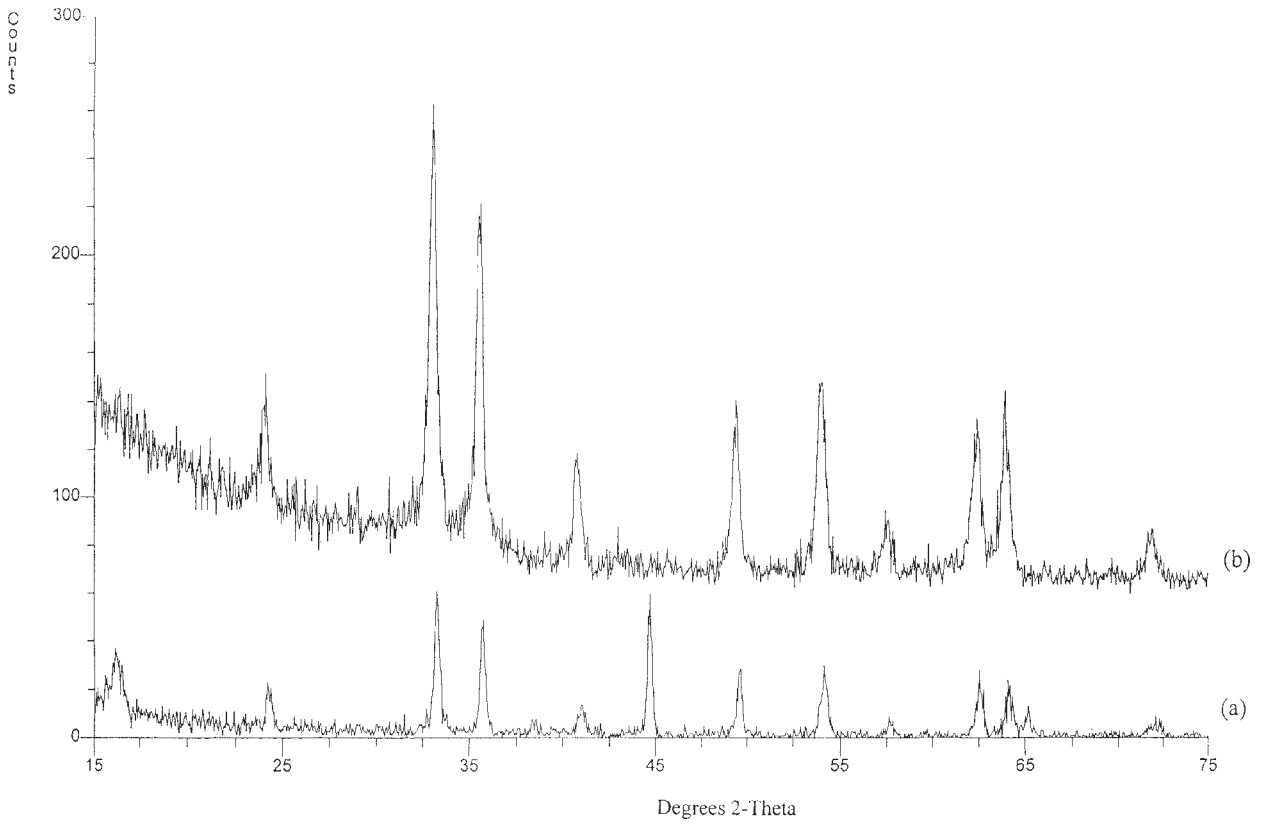

Figure 4. Powder X-ray diffraction pattern of (a) H_2O/Fe_2O_3(F) and (b) SO_4^{2-}/Fe_2O_3(F).

Table 2
Powder X-ray diffraction line widths for pre-reactor non-sulfated and sulfated haematite derived from goethite.

Reflection	Width[a] (2θ)	
	H_2O/Fe_2O_3	SO_4^{2-}/Fe_2O_3
(012)	0.35	0.50
(104)	0.30	0.70
(110)	0.20	0.30
(006)	0.15	0.30
(113)	0.30	0.40
(202)	0.30	0.20
(024)	0.25	0.70
(116)	0.30	0.60
(018)	0.40	1.00
(214)	0.20	0.50
(300)	0.20	0.15
(1010)/(119)	0.25	1.00

[a] α_2-stripped.

tween H_2O/Fe_2O_3(G) and H_2O/Fe_2O_3(F) materials relates to differences in morphology or phase. The poorer catalytic performance of the H_2O/Fe_2O_3(F) samples may simply be due to the lower content of crystalline haematite, as may the observation that SO_4^{2-}/Fe_2O_3(G) has a higher specific activity than SO_4^{2-}/Fe_2O_3(F). However, the effects of sulfation on both systems, which are general, cannot be explained so easily. The inhibition of total oxidation at lower temperatures suggests that there are a number of sites which are poisoned. It is probable that these are Fe^{3+} cations which are simply blocked by SO_4^{2-} complexation. At higher temperature, another type of site appears to be operative. On the basis of the marked enhancement in specific activity for the Fe_2O_3(F) system, it appears to be directly related to the presence of SO_4^{2-}, and may even be sulfate itself. The smaller effect on activity in the case of Fe_2O_3(G) may, therefore, correspond with the lower sulfate adsorption capacity of goethite [19] and the lower surface area of our goethite precursor (40 $m^2\,g^{-1}$), compared to 2-line ferrihydrite (234 $m^2\,g^{-1}$). In view of the fact that the materials were calcined above the reaction temperature prior to reactor testing, we consider it unlikely that sulfate decomposition during reaction is contributing to catalytic performance. The relationship between catalytic activity and sulfur content is currently under investigation. The observation of selective oxidation products in the case of the sulfated materials at 500 °C is most likely a reflection of the higher oxygen conversion.

Acknowledgement

It is a pleasure to record our appreciation of the assistance Drs. David Williams and Michael Crapper (Department of Physics, University of Loughborough) for allowing us to use their powder X-ray diffractometer, Mr. D. Lacey (Faculty of Science and Mathematics, Nottingham Trent University) for TEM studies, Professor Richard Joyner and Dr. Michael Stockenhuber (Department of Chemistry and Physics, Nottingham Trent University) for useful discussions.

References

[1] K. Arata and M. Hino, Mater. Chem. Phys. 26 (1990) 213.
[2] V. Adeeva, J.W. de Haan, J. Jänchen, G.D. Lei, V. Schumann, L.J.M. van de Ven, W.H.M. Sachtler and R.A. van Santen, J. Catal. 151 (1995) 364.
[3] D. Fărcaşiu, A. Ghenciu and J.Q. Li, J. Catal. 158 (1996) 116.
[4] X. Song and A. Sayari, Catal. Rev. Sci. Eng. 38(3) (1996) 329.
[5] T.J. Hall, J.S.J. Hargreaves, G.J. Hutchings, R.W. Joyner and S.H. Taylor, Fuel Proc. Technol. 42 (1995) 151.
[6] C.-H. Lin and C.-Y. Hsu, J. Chem. Soc. Chem. Commun. (1992) 1479.
[7] K. Murata, T. Hayakawa and K.I. Fujita, Chem. Commun. (1997) 221.
[8] P. Batamack, I. Bucsi, Á. Molnár and G.A. Olah, Catal. Lett. 25 (1994) 11.
[9] T.R. Baldwin, R. Burch, G.D. Squire and S.C. Tsang, Appl. Catal. 74 (1991) 137.
[10] C. Sarzanini, G. Sacchero, F. Pinna, M. Signoretto, G. Cerrato and C. Morterra, J. Mater. Chem. 5 (1995) 353.
[11] D. Fărcaşiu and J.Q. Li, Appl. Catal. A 128 (1995) 97.
[12] R.M. Cornell and U. Schwertmann, *The Iron Oxides* (VCH, Weinheim, 1996).
[13] R.M. Cornell, A.M. Posner and J.P. Quirk, J. Inorg. Nucl. Chem. 36 (1974) 1937.
[14] T. Yamaguchi and T. Takahashi, Comm. Am. Ceram. Soc. (1982) C83.
[15] K. Nakamoto, *Infrared and Raman Spectra of Inorganic and Coordination Compounds* (Wiley, New York, 1986).
[16] R.L. Parfitt and R.St.C. Smart, J. Chem. Soc. Faraday Trans. 1 (1977) 796.
[17] G. Brown, in: *Associated Minerals*, eds. G.W. Brindley and G. Brown, Crystal Structures of Clay Minerals and Their X-Ray Identification (Min. Soc., London) p. 361.
[18] K. Arata, Appl. Catal. A 146 (1996) 3.
[19] R.L. Parfitt and R.St.C. Smart, Soil Sci. Soc. Am. J. 42 (1978) 48.